A Novel Approach for Motion Artifact Reduction in PPG Signals Based on AS-LMS Adaptive Filter

Ashoka Reddy

IEEE Transactions on Instrumentation and Measurement

A Novel Approach for Motion Artifact Reduction in PPG Signals Based on AS-LMS Adaptive Filter

M. Raghu Ram, *Member, IEEE*, K. Venu Madhav, *Member, IEEE*, E. Hari Krishna, *Member, IEEE*, Nagarjuna Reddy Komalla, and K. Ashoka Reddy, *Member, IEEE*

***Abstract*—The performance of pulse oximeters is highly influenced by motion artifacts (MAs) in photoplethysmographic (PPG) signals. In this paper, we propose a simple and efficient approach based on adaptive step-size least mean squares (AS-LMS) adaptive filter for reducing MA in corrupted PPG signals. The presented method is an extension to our prior work on efficient use of adaptive filters for reduction of MA in PPG signals. The novelty of the method lies in the fact that a synthetic noise reference signal for an adaptive filtering process, representing MA noise, is generated internally from the MA-corrupted PPG signal itself instead of using any additional hardware such as accelerometer or source–detector pair for acquiring noise reference signal. Thus, the generated noise reference signal is then applied to the AS-LMS adaptive filter for artifact removal. While experimental results proved the efficacy of the proposed scheme, the merit of the method is clearly demonstrated using convergence and correlation analysis, thus making it best suitable for present-day pulse oximeters utilizing PPG sensor head with a single pair of source and detector, which does not have any extra hardware meant for capturing noise reference signal. In addition to arterial oxygen saturation (SpO_2) estimation, the artifact reduction method facilitated the waveform contour analysis on artifact-reduced PPG, and the conventional parameters were evaluated for assessing the arterial stiffness.**

***Index Terms*—Adaptive step-size least mean squares (AS-LMS) adaptive filter, motion artifact (MA), oxygen saturation, photoplethysmographic (PPG) signal, pulse oximeter.**

I. Introduction

A PULSE oximeter has become a standard monitor during critical care for noninvasive continuous monitoring of arterial-blood oxygen saturation (SaO_2) and pulse rate (PR) [1]. When SaO_2 is estimated using a pulse oximeter, it is denoted as SpO_2. A pulse oximeter makes use of photoplethysmographic (PPG) signals acquired at red and infrared (IR) wavelengths with the help of suitable sensors attached to the finger/earlobe/forehead of the subject [2]. A PPG sensor can be of transmission or reflection type, consisting of matched LED (source)–photodiode (detector) pair, and depends on the principles of transmission, absorption, and dispersion of light for its operation, as light passes through different absorbing substances such as skin pigmentation, biological tissue, bone, arterial and venous blood. A typical PPG signal contains two components. The first one is a large dc component, due to constant absorption of light when passing through the skin–tissue–bone. The second one is a small ac component at PR, due to the component of light passing through pulsating arteries caused by the heartbeat [3], [4]. A pulse oximeter needs red and IR PPG signals with clearly separable dc and ac parts for error-free SpO_2 estimation. However, PPGs are usually corrupted by motion artifacts (MAs) due to voluntary or involuntary movements of the subject while acquiring the data. Since the pulsatile component is quite small in a PPG (0.1% of total signal amplitude), even a slightest movement of the patient will lead to MA, resulting in inaccurate estimation of SpO_2. Reduction of MA in PPG signals for reliable estimation of SpO_2 has been, in fact, a challenging problem ever since the invention of pulse oximetry. The effect of MA on SpO_2 can be reduced by suitable processing of PPG signals. To some extent, it can be reduced by displaying the average value of several SpO_2 readings. There have been many attempts to reduce the influence of MAs on corrupted PPG signals. Moving average method is commonly employed for the reduction of MA [2], [5], and it works well for only a limited range of artifacts. In-band noise results when the spectra of MA and that of the PPG signal overlap significantly. Adaptive filters, which effectively deal with in-band noise [6]–[9], need a reference signal that is strongly correlated either with the artifact but uncorrelated with the signal or with the signal but uncorrelated with the artifact. In most cases, suitable reference signals, representing MA, were obtained by employing additional hardware. For example, reference signals were obtained from an additional transducer attached to sense the movement [6], [7] or by employing an additional reflectance-type optoelectronic sensor [8]. Use of a synthetic reference signal estimated from the artifact-free part of the PPG signal [9] was also reported for reducing MA. In the Masimo SET [10], venous-blood volume changes are identified as a significant contributor to noise during motion, and hence, a venous noise reference signal is extracted from the artifact-induced PPG signal itself, without extra hardware. The added artifact is then removed from the PPG signal using adaptive noise cancellation. A signal processing technique using multirate filter bank with a matched filter [11] performed better compared to the moving average

Manuscript received June 20, 2011; revised August 28, 2011; accepted September 1, 2011. Date of publication December 22, 2011; date of current version April 6, 2012. The Associate Editor coordinating the review process for this paper was Dr. José Pereira.

M. R. Ram, K. V. Madhav, and K. A. Reddy are with the Department of Electronics and Instrumentation Engineering, Kakatiya Institute of Technology and Science, Warangal 506015, India (e-mail: reddy.ashok@yahoo.com).

E. H. Krishna is with the Department of Electronics and Communication Engineering, KU College of Engineering and Technology, Kakatiya University, Warangal 506009, India.

N. R. Komalla is with the Department of Anaesthesiology, Govt. MGM Hospitals, Warangal 506007, India.

Color versions of one or more of the figures in this paper are available online at http://ieeexplore.ieee.org.

Digital Object Identifier 10.1109/TIM.2011.2175832

approach. The dynamic nature of the biological systems causes most biological signals to be nonstationary and change substantially in their properties over time. Based on this nonstationary nature of PPG signals, time–frequency methods like wavelet transforms [12] and smoothed pseudo Wigner–Ville distribution [13] were applied on PPG signals showing significant improvements compared to traditional approaches. A model-based artifact reduction methodology [14] was proposed with a nonlinear optical receiver based upon inversion of a physical artifact model and was implemented [15] utilizing an additional source–detector pair, resulting in the three-wavelength probe, for reduction of MA. By exploiting the independence between PPG and MA signals, it was also demonstrated that MAs were reduced by using independent component analysis (ICA). While the third-order ICA of the time derivative of PPG signals resulted in better artifact suppression [16], the ICA applied with a preprocessing called block interleaving with low-pass filtering performed better than ICA alone [17]. A comparative study on the efficacy of wavelet transform and adaptive filtering techniques in restoring the artifact-reduced PPG signals [18], [19] for estimation of heart rate (HR) and pulse transit time revealed that both methods introduce phase shifts to the PPG signals. New processing methods addressing MA reduction, based on singular value decomposition (SVD) [20], cycle-by-cycle Fourier series analysis [21], and higher order statistics [22], extracted clean artifact-free PPG signals preserving all the essential morphological features required.

Other approaches for reducing MA in PPG signals include adaptive filtering and improvements in mechanical design and sensor configuration [28]. Of which, motion-tolerant wearable biosensors using MEMS accelerometers [29], [30] based on adaptive noise cancellation utilizing accelerometer reference have motivated the researchers to think in the direction of improving sensor design. However, the MA reduction algorithms developed around adaptive filters require that a reference signal that is strongly correlated either with the artifact but uncorrelated with the signal or with the signal but uncorrelated with the artifact be available. Hence, these methods invariably depend on additional hardware such as accelerometer [29], [30] or source–detector pair [15] for acquiring noise reference signal, resulting in a three-wavelength probe as opposed to a two-wavelength probe of commercial pulse oximeter (CPO). Using dedicated hardware for obtaining noise reference, for example, accelerometer, in fact, resulted in efficient noise reduction in PPG signals [30]. However, the work reported in this paper is mainly aimed at implementing an adaptive filtering algorithm for MA reduction, making use of existing two-wavelength probe of CPO without looking for any additional hardware.

This technique is based on extension of our prior work on efficient use of adaptive filters for reduction of MA in PPG signals [23]–[25]. The novelty of the proposed technique lies in the fact that a synthetic noise reference signal for an adaptive filtering process, representing MA noise, is generated internally from the MA-corrupted PPG signal itself instead of using any additional hardware such as accelerometer or additional source–detector pair for acquiring noise reference signal. In [25],[1] the synthetic noise reference was generated using the well-known fast Fourier transform (FFT) technique. In this paper, we present two more methods, i.e., one using SVD and another using ICA for the generation of MA noise reference signal. Subsequently, the noise references generated by the aforesaid methods are tested for their correlation with the MA noise component using randomness parameter calculations. Based on the randomness deviation, the best suitable noise reference signal is selected and then applied to the proposed adaptive step-size least mean squares (AS-LMS) adaptive filter. The performance of the proposed scheme is studied by: 1) comparing the AS-LMS scheme of artifact reduction with time-varying step-size LMS (TVS-LMS)- and constant step-size LMS (CS-LMS)-based adaptive algorithms and 2) computing SpO_2 using both time-domain (TD) and frequency-domain (FD) analyses of PPG signals.

II. MA Reduction

The frequency spectrum of noise due to MA (0.1 Hz or more) has every chance of overlapping with that of a useful PPG signal (0.5–4.0 Hz) and results in in-band noise. Adaptive filters are very effective in in-band noise cancellation by self-adjusting the filter coefficients based on some specific adaptive algorithms. In addition to the suitable adaptive algorithm, the reference signal plays a vital role in adaptive filters. In fact, the adaptive filters require a reference signal $[N_R(n)]$ that is strongly correlated either with the artifact but uncorrelated with the signal or with the signal but uncorrelated with the artifact. The proposed scheme of MA reduction showing an efficient synthetic noise reference signal generating section and an AS-LMS adaptive filtering section is illustrated in the form of a block diagram shown in Fig. 1.

A. Synthetic Noise Reference Signal $[N_R(n)]$ Generation

This constitutes the novel part of the proposed method. Here, a synthetic $N_R(n)$ is internally generated for use in the proposed adaptive filtering technique without using any extra hardware such as accelerometer or additional source–detector pair for acquiring $N_R(n)$, as was normally done [6]–[8].

$N_R(n)$ is generated from the corrupted PPG signal individually using three different methods, namely, FFT, ICA and SVD, as illustrated hereinafter.

1) ***FFT method:*** The steps involved in generating the noise reference signal using the FFT method [25] are described next.
   a) The frequency spectrum of the MA-corrupted PPG signal consisting of various frequency components, viz., the pulsatile PPG cardiac portion (0.5–4 Hz), respiratory activity (0.2–0.35 Hz), and MA noise component (0.1 Hz or more) information, is computed.
   b) By setting the coefficients of cardiac and respiratory frequency components in the spectrum of the

[1]The material in this paper was presented at the 2011 IEEE International Instrumentation and Measurement Technology (I^2MTC) Conference, Hangzhou, China, May 10–12, 2011.

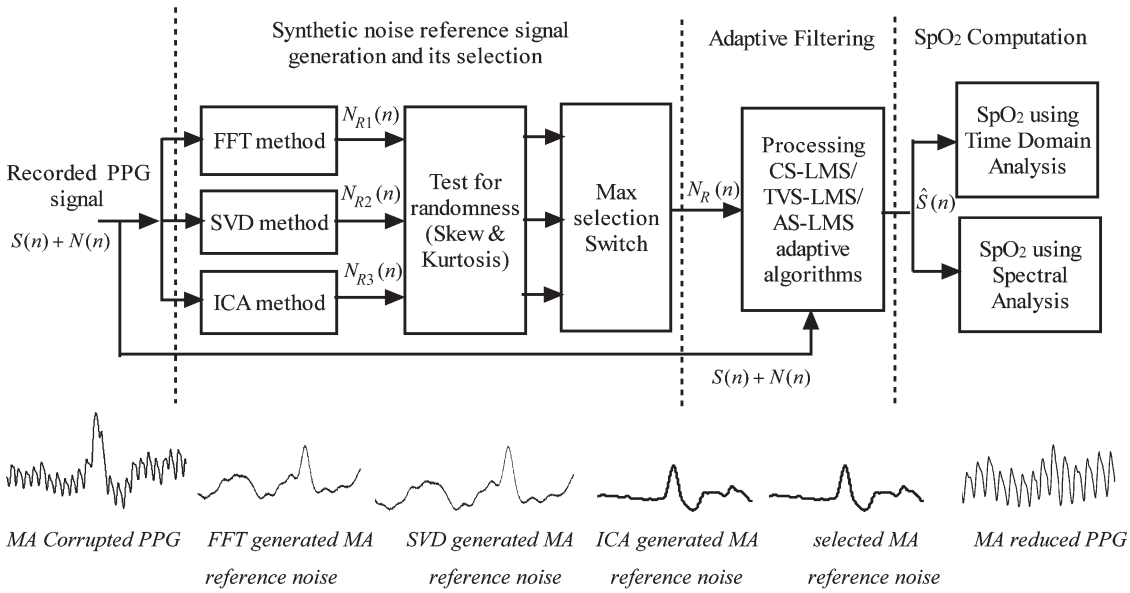

Fig. 1. Block diagram of the proposed MA reduction scheme. The noise reference generating block takes the MA $[N(n)]$ corrupted PPG signal $[(Sn) + N(n)]$ and gives the best possible noise reference $[N_R(n)]$ representing MA. The proposed adaptive algorithm operates on $N_R(n)$ and $(Sn) + N(n)$ to recover the PPG from MA. Finally, SpO_2 is computed using TD and FD analysis methods.

MA-corrupted PPG signal to zero, a modified spectrum corresponding to noise is obtained.

c) By applying inverse Fourier transform to this modified noise spectrum, a synthetic noise reference signal, representing MA, is generated.

2) ***SVD method:*** SVD is an important tool of linear algebra. Once decomposed, the singular values of a given data matrix contains information about the noise level in the data [20]. The steps involved in generating the noise reference signal using the SVD method are described as follows.
   a) SVD is applied to the aligned PPG data matrix of the recorded signal, and the ratio of the first two singular values, called singular value ratio (SVR), is computed.
   b) In each case, the length of the signal is considered as a period for the expected range of HRs. The SVR values are then plotted against the periods to obtain the graph called SVR spectrum of the signal.
   c) From the SVR spectrum, the particular value of the period for which SVR is maximum is considered as the period of the PPG signal.
   d) Now, the data matrix is realigned based on the periodicity computed from the SVR spectrum.
   e) SVD is applied again to the realigned PPG data matrix in which the first two singular values representing the pulsatile and respiratory components, respectively, are made zero.
   f) The noise reference signal is generated from the retained singular values of the realigned PPG data matrix.
3) ***ICA method:*** ICA is a quite-powerful signal processing technique [17], which expresses a set of random variables as linear combination of statistically independent component variables. The steps involved in generating the noise reference signal using the ICA method are described next.
   a) The preprocessing consists of low-pass filtering with a cutoff frequency of 10 Hz to eliminate the high-frequency noise components from the recorded PPG signal.
   b) The preprocessed red and IR PPG signals are then downsampled until it eliminates the pulsatile component of the PPG signal while keeping the respiratory and MA components intact.
   c) The ICA algorithm is applied to separate the linearly mixed respiratory and MA signals, in which the MA signal can be referred to as generated noise reference signal.

MAs are mainly due to the voluntary or involuntary vibrations of the examinees [31], because of which the cardiac synchronous pulsatile component of the arterial blood will be swamped by the artifact. Hence, the much useful pulsatile component of PPG gets corrupted by random fluctuations of the arterial blood in majority of the cases, resulting in changed morphology of the PPG signal. Hence, randomness measures like skew and kurtosis could serve as important features for detection of MA.

By definition, skew is a measure of the symmetry (or the lack of it) of a probability distribution, while the kurtosis measure indicates a heavy tail and peakedness or a light tail and flatness of a distribution relative to the normal distribution. It captures the random variations of data from the mean. The skew and kurtosis of a random variable "x" are given by

$$\text{skew}: \quad C_{3x}(0,0) = \frac{\mu_3}{\sigma^{3/2}} \tag{1}$$

$$\text{kurtosis}: \quad C_{4x}(0,0) = \frac{\mu_4}{\sigma^4} - 3 \tag{2}$$

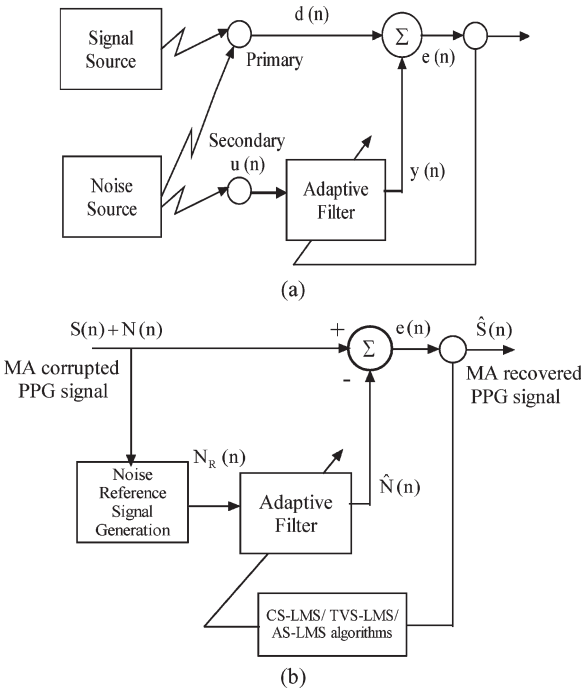

Fig. 2. (a) Block diagram of a basic adaptive filter. (b) MA reduction configuration for the proposed scheme, where the noise reference signal $N_R(n)$ is generated from the MA-corrupted PPG $[S(n) + N(n)]$ and applied to the adaptive filter based on the AS-LMS algorithm, which, in turn, estimates the noise $\hat{N}\ (n)$.

where σ is the standard deviation and μ_3 and μ_4 are the third and fourth central moments, respectively. A suitable MA noise reference will be selected for adaptive filtering based on the calculated skew and kurtosis for the signals generated by the said methods. Although the criterion used for the selection of the best synthetic noise reference signal generated (individually by using FFT, SVD, and ICA methods) is the method which yields the noise reference signal with the highest values for both skew and kurtosis, it has also been demonstrated in Section IV that a high value of kurtosis alone would serve as a reliable measure for the selection of synthetic noise reference signal.

B. MA Reduction Using AS-LMS Technique

The basic form of an adaptive filter is shown in Fig. 2(a), wherein the scheme looks for a reference signal, which requires additional hardware facility. The structure of the proposed adaptive filtering scheme is shown in Fig. 2(b), which uses existing two-wavelength probe of CPO without looking for any additional hardware. The LMS algorithm is the most popular one [26], and our previous work [23]–[25] exploited its usefulness in CS-LMS and TVS-LMS algorithms for MA reduction. We present, in this paper, the proposed AS-LMS algorithm to recover the artifact-free PPG from the MA-corrupted signal. The filtering and weight update equations for each of the algorithms are detailed hereinafter.

C. Noise Model

In the academia, efficient algorithms based on adaptive filtering have been developed to address the MA reduction problem. It is clearly evident from the researchers' view that adaptive filters can be efficiently utilized for any PPG system designed using different signal distortion models [28]–[30]. Adaptive filters effectively reduce MAs whether they are random or periodic in nature. In this adaptive filtering case, an additive distortion model [29], [30] is assumed, in which the motion-corrupted PPG signal is considered to be a mixture of clean (original) PPG and MA. In addition, the artifact is assumed to be highly uncorrelated with the useful PPG signal.

1) CS-LMS Algorithm

The CS-LMS algorithm, which makes use of instantaneous estimate of the gradient to search the minimum of the error surface, can be described using the following three equations:

$$y(n) = w^T(n)u(n) : \text{Filter output} \tag{3}$$

$$e(n) = d(n) - y(n) : \text{Error formation} \tag{4}$$

$$w(n+1) = w(n) + \mu e(n)u(n) : \text{Weight vector update} \tag{5}$$

where $u(n)$ is the filter input, $e(n)$ is the error incurred by the adaptive filter, $d(n)$ is the desired output of the filter, and μ is the step size used in weight vector updation.

2) TVS-LMS algorithm

Selection of CS parameter (μ), which controls stability and convergence speed, is very critical in the case of the simple CS-LMS algorithm. In order to improve the characteristics of an LMS-based adaptive filter, the TVS-LMS algorithm may be employed. The complete algorithm can be described using the following equations:

$$y(n) = w^T(n)u(n) : \text{Filter output} \tag{6}$$

$$e(n) = d(n) - y(n) : \text{Error formation} \tag{7}$$

$$w(n+1) = w(n) + \mu_n e(n)u(n) : \text{Weight vector update} \tag{8}$$

$$\mu_n = \alpha_n \times \mu_0 : \text{TVS} \tag{9}$$

$$\alpha_n = C^{1/(1+a^n b)} : \text{Decaying factor} \tag{10}$$

where C, a, b are positive constants that will determine the magnitude and rate of decrease of α_n. Accordingly, C has to be a positive number larger than one, when $C = 1$, α_n will be equal to one, a new algorithm will be the same as the conventional LMS algorithm, and μ_0 is the initial step size.

3) AS-LMS algorithm

In a nonstationary environment, the minimum cost function $(J_{\min})$ takes a time-varying form, and step size control plays an important role in the variability of the estimates and algorithm convergence time. Furthermore, due to the presence of gradient noise in the LMS algorithm, the tap weight vector follows a Brownian movement around the minimum point of error performance rather than terminating on the Weiner solution. The AS-LMS algorithm is developed similar to CS-LMS; a fourth

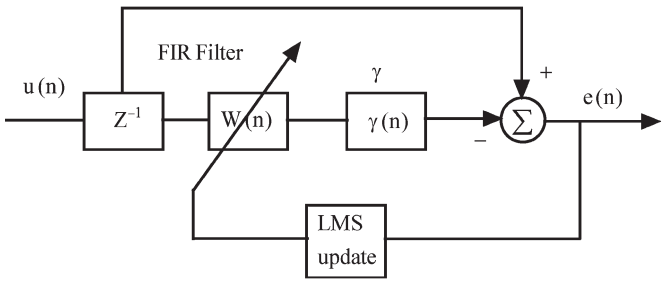

Fig. 3. Weight update mechanism in the AS-LMS adaptive filter.

equation is added to the set of three LMS equations (3)–(5) to adaptively update the step size parameter

$$\mu(n+1) = \mu(n) + \rho e(n)\gamma^H(n)u(n) \tag{11}$$

where γ^H is the gradient vector defined as the partial derivative of the weight vector at a sample (iteration) with respect to the step size parameter of the same sample

$$\gamma(n) = \partial w(n)/\partial \mu(n) \tag{12}$$

and ρ is a small positive constant which controls the update of the step size parameter. The weight update mechanism is shown in Fig. 3.

Inclusion of gradient vector results in better tracking performance in terms of convergence time by updating the step size parameter and then reducing the error estimate in each iteration.

As per the adaptive filter block diagram shown in Fig. 2(b), by efficiently processing both the generated synthetic noise reference signal data and the MA-corrupted PPG signal information using any LMS adaptive algorithm, the MA-recovered PPG signal can be obtained. The necessary equations to implement the proposed method are given as follows:

$$\hat{S}(n) = S(n) + N(n) - \hat{N}(n) \tag{13}$$

$$\hat{N}(n) = \sum_{i=0}^{L} w_i N_R(n-i) \tag{14}$$

$$w_i(n+1) = w_i(n) + \mu_n S(n) N_R(n-i) \tag{15}$$

where i: 0, 1, 2, …, L; L: filter order; $S(n)+N(n)$: MA-corrupted PPG signal; $\hat{S}(n) = e(n)$: MA-recovered PPG signal; $\hat{N}(n)$: estimated noise reference signal; and $N_R(n)$: synthetic noise reference signal.

III. Data Acquisition

A clip-on-type PPG sensor, housing a red LED and an IR LED on one side and a photodiode detector on the other side, was designed and developed to record PPG signals from different subjects and was interfaced to the signal conditioning circuitry, as shown in Fig. 4. The red and IR PPG signals (samples of red and IR detector voltages) were acquired, at a sampling rate of 200 Hz, using the NI-DAQPad-6015 data acquisition system manufactured by National Instruments.

To evaluate the performance of the proposed method, frequently encountered artifacts during postoperative recovery and intensive care were created intentionally during the PPG data recording process. The experimental protocol followed for recording the data is as follows.

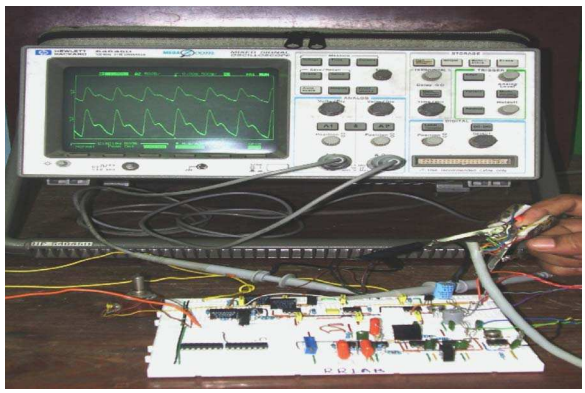

Fig. 4. Developed prototype for PPG analog front end.

1) The transmission-type PPG sensor was connected to the left hand of the subject.
2) Red and IR PPGs are recorded for a span of 4 min.
3) Initial 1 min of PPG was recorded without MA by keeping the finger, connected to the sensor probe, at rest.
4) At the end of the first minute, the volunteer was asked to intentionally introduce the artifact by moving the finger in a particular direction, for example, vertical for 2 min.
5) Recording ended with a final 1-min period, wherein the finger was again kept at rest without any motion.

This protocol was repeated on each subject for each of the following three movements which are encountered in reality, namely, 1) vertical motion; 2) horizontal motion; and 3) bending motion of the finger. The experimental procedure adopted while recording the PPG data was approved by the Ethics Committee of the Indian Institute of Technology, Madras, and the PPG data were collected after obtaining "informed consent" from all the volunteers.

IV. Results and Discussion

The recorded PPG data were processed and analyzed using the MATLAB signal processing toolbox. A typical PPG signal corrupted with the horizontal motion of the finger is shown in Fig. 5. The computed spectra of MA-corrupted and MA-recovered PPGs are shown in Fig. 6 for frequency information of the various components included in the PPG, i.e., pulsatile cardiac portion (0.5–4 Hz), respiratory activity (0.2–0.35 Hz), and MA noise component (0.1 Hz or more).

A. MA Noise Reference Signal $[N_R(n)]$ Generation

Initially, noise reference signals were generated using FFT, SVD, and ICA methods, as discussed in Section II-A, from the PPG data recorded for typical motions of the finger. Fig. 7(a1)–(d1) shows the extracted MA noise for the vertical motion of the finger. Similar ones are plotted for the bending motion of the finger in Fig. 8 and for the horizontal motion of the finger in Fig. 9.

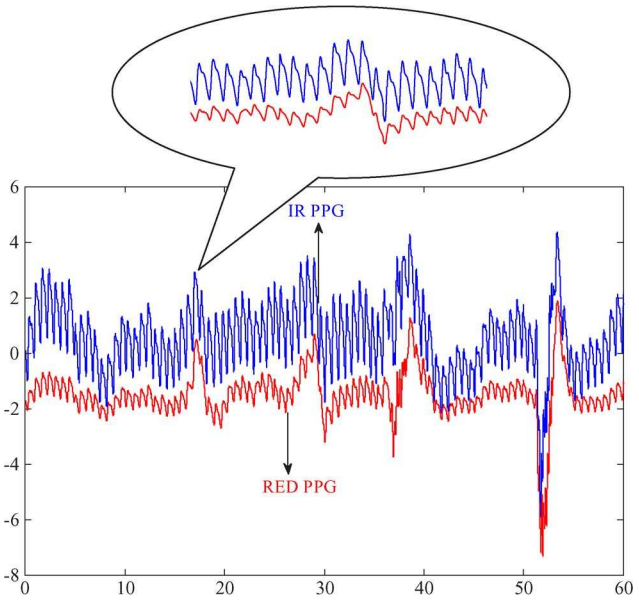

Fig. 5. Recorded PPG data comprising MA noise of the volunteer.

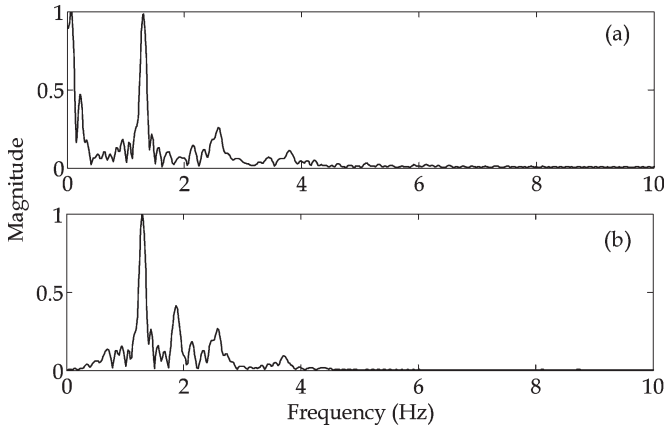

Fig. 6. Computed spectra of MA-corrupted PPG in (a) and of MA-recovered PPG in (b) showing absence of MA in the spectrum.

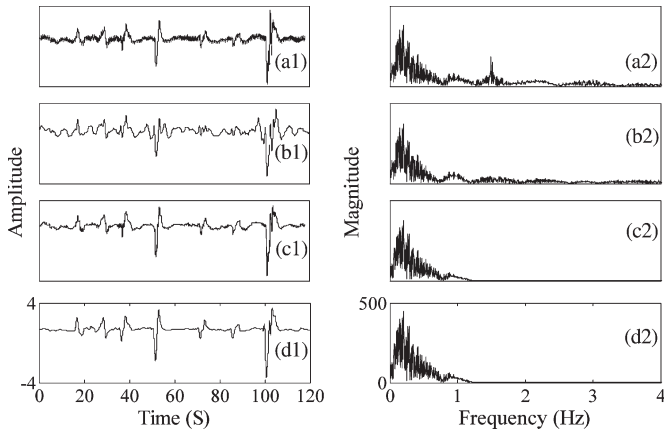

Fig. 7. (a1)–(d1) Recorded PPG signal for "vertical motion of finger"; synthetic noise reference signal generated using FFT, SVD, and ICA methods; and their corresponding spectra in (a2)–(d2), respectively.

To decide on the criterion for the selection of the best synthetic noise reference signal generated (individually by using FFT, SVD, and ICA methods), a thorough analysis

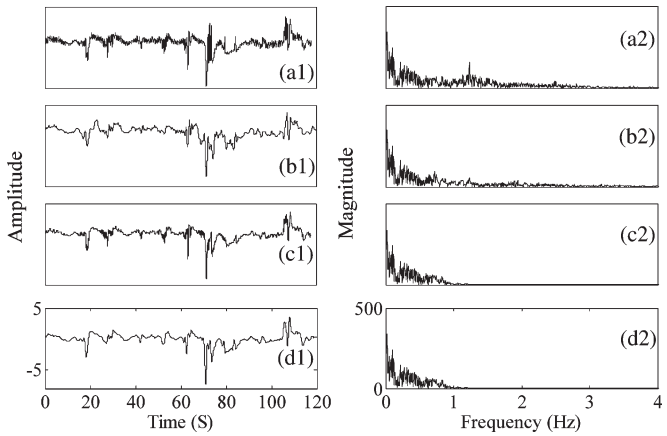

Fig. 8. (a1)–(d1) Recorded PPG signal for "bending motion of finger"; synthetic noise reference signal generated using FFT, SVD, and ICA methods; and their corresponding spectra in (a2)–(d2), respectively.

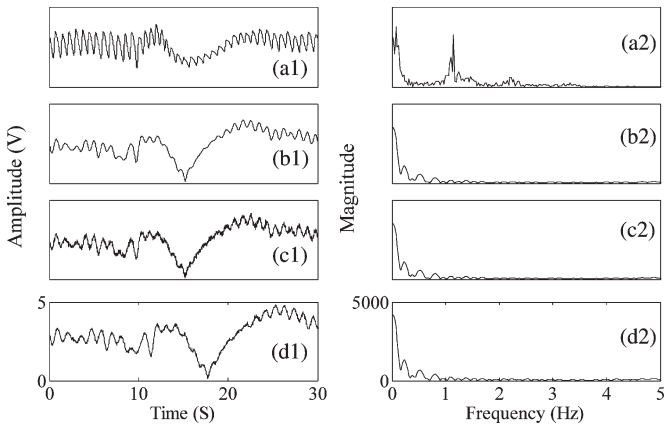

Fig. 9. (a1)–(d1) Recorded PPG signal for "horizontal motion of finger"; synthetic noise reference signal generated using FFT, SVD, and ICA methods; and their corresponding spectra in (a2)–(d2), respectively.

was carried out by computing skew (Sk) and kurtosis (Ku) values for: 1) clean section of PPG signal; 2) MA-corrupted and MA-recovered sections of PPG; 3) FFT-generated synthetic reference noise signal;4) SVD-generated synthetic reference noise signal; and 5) ICA-generated synthetic reference noise signal.

The previous analysis was carried out for all the PPGs with frequently encountered MA (vertical, horizontal, and bending motions), and results are presented in the form of Table I. *Of the three methods employed for MA reference noise generation, the calculated randomness parameters (skew and kurtosis), as tabulated in* Table I, *clearly indicate that the ICA-generated MA reference is the best one for use as reference yielding the highest values for both skew and kurtosis.*

The following observations can be made from Table I:

1) It is important to note that the values of skew and kurtosis will vary with the type of MA.
2) It can be clearly observed from Table I that both of these measures for MA-corrupted PPGs are higher in magnitude when compared to the same measures for clean PPG data.
3) Of skew and kurtosis, the kurtosis resulted in a much higher value than the skew for MA-corrupted segments. *Hence, even though both skew and kurtosis are higher in*

TABLE I
COMPUTED RANDOMNESS PARAMETERS IN TERMS OF SKEW AND KURTOSIS FOR SELECTION OF THE BEST GENERATED SYNTHETIC NOISE REFERENCE SIGNALS

PPG	Horizontal motion		Vertical motion		Bending motion	
	Sk	***Ku***	***Sk***	***Ku***	***Sk***	***Ku***
Clean section	2.15	6.98	1.38	7.53	0.76	6.73
MA section	**3.95**	**21.73**	**3.14**	**17.95**	**1.95**	**15.45**
Noise ref. from FFT Method	3.16	20.82	2.74	15.75	1.83	11.07
Noise ref. from SVD Method	3.62	21.22	2.92	17.04	1.87	14.41
Noise ref. from ICA Method	**3.86**	**21.46**	**2.98**	**17.46**	**1.91**	**14.83**
MA reduced section	2.28	7.19	1.47	7.65	0.89	6.93

magnitude, a high value of kurtosis alone would serve as a reliable measure for the selection of noise reference.

4) The Sk and Ku values of the noise reference derived from the ICA-based method are very close to the MA-corrupted sections of the same PPG signal. Hence, the ICA-based noise reference may be taken as a closely matched noise reference signal for adaptive filtering purposes.
5) In all the cases, the randomness parameter Sk and Ku values of the noise reference derived from the ICA-based method are maximum compared to the FFT- and SVD-based methods.
6) Moreover, it is worth noting that for all kinds of MAs, the randomness parameters calculated for the PPG signals processed using the AS-LMS adaptive filter (MA-reduced sections) are very close to the clean PPG sections, indicating the efficacy of the presented method.

In addition, correlation analysis of skew and kurtosis with clean and MA sections was also performed by calculating correlation coefficient (r) and confidence level (p), which yielded the information about statistical dependence of various sections, and the results are tabulated in Table II. If the confidence level $p < 0.05$, then the correlation is very much significant. It can be seen that the generated noise reference is strongly correlated with the MA section and that the correlation is maximum for the noise reference generated using the ICA-based method.

To demonstrate the MA noise correlation with respect to the generated noise reference for frequently encountered MAs, correlation analysis is tested in terms of intraclass correlation coefficients to characterize the signal nature. Correlation analysis (r values) of the generated noise reference signals with clean and MA sections for different MAs, presented in Table III, emphasizes again the superiority of the ICA-based noise reference signal.

Since the systemic heart pulsations of the PPG signal have a very little correlation with the physical moment for the MA signal [16], [17], the PPG and MA signals are assumed to be statistically independent of each other. Hence, the MA-corrupted red and IR PPG signals, when processed using ICA, yielded the best noise reference by virtue of the source separation property of ICA from linearly mixed signals.

TABLE II
COMPUTED CORRELATION COEFFICIENT AND CONFIDENCE LEVEL FOR MA-REDUCED PPG AND NOISE REFERENCE SIGNALS

Correlation of skews	Clean section	MA section
Noise reference using FFT	r=0.2756 p=0.7265	r=0.9950 p=0.0639
Noise reference using SVD	r=0.1865 p=0.8659	r=0.9951 p=0.003
Noise reference using ICA	r=0.1875 p=0.86	r=0.9986 p=0.03
MA recovered using AS-LMS Adaptive filter	r=0.9995 p=0.021	r=0.2376 p=0.8424
Correlation of kurtosis	**Clean section**	**MA section**
Noise reference using FFT	r=0.2834 p=0.8171	r=0.9956 p=0.0599
Noise reference using SVD	r=0.1788 p=0.8856	r=0.9999 p=0.008
Noise reference using ICA	r=0.1905 p=0.878	r=1.000 p=0.001
MA recovered using AS-LMS Adaptive filter	r=0.9985 p=0.034	r=0.2429 p=0.8356

B. MA Reduction Using AS-LMS Algorithm

Once the best MA noise reference $[N_R(n)]$ is generated from the MA-corrupted PPG itself, the immediate next step is to use this $N_R(n)$ in the adaptive filtering scheme. Before application of the proposed MA reduction AS-LMS algorithm, its performance was evaluated in terms of convergence rate as an mean square error (MSE) measure with respect to the number of iterations. The performance curves shown in Fig. 10 clearly indicate that *the AS-LMS algorithm has faster convergence rate with minimum MSE.* Hence, the MA-corrupted PPG signals are now processed with the proposed AS-LMS algorithm.

In general, MAs completely disturb the morphology of the PPG signal. The proposed AS-LMS algorithm efficiently reduces MA and thus preserves the PPG signal morphology. In addition, the PPG signal is also affected by other kinds of noise such as skin pigmentation, individual tissue characteristics,

TABLE III
COMPUTED CORRELATION COEFFICIENTS FOR DIFFERENT MOTIONS OF FINGER

Correlation of Noise reference	Vertical motion		Bending motion		Horizontal motion	
	MA section	Clean section	MA section	Clean section	MA section	Clean section
using FFT	0.6870	0.286	0.6968	0.265	0.6754	0.259
using SVD	0.7525	0.254	0.7848	0.297	0.7961	0.286
using ICA	0.9304	0.239	0.9104	0.229	0.9247	0.212

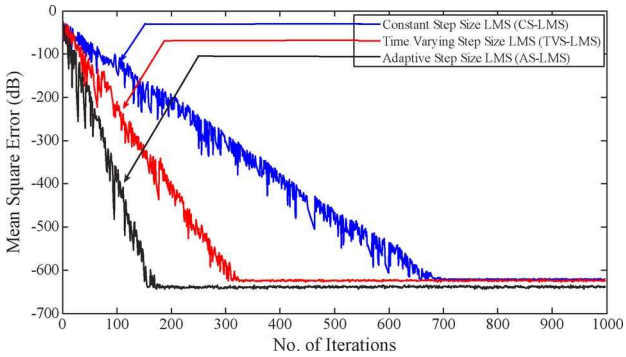

Fig. 10. Convergence study: mse against number of iterations.

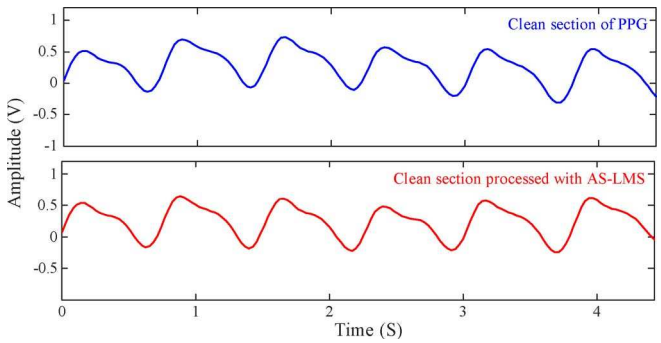

Fig. 11. Clean sections of (top trace) PPG and (bottom trace) processed PPG showing the morphology retention capacity of the method.

peripheral circulation, and initial blood flow in the measured area, which mostly affect the dc component and not the pulsatile component. Suitable corrective measures have been suggested in the literature [27] for minimizing the influence of those kinds of noise which affect the baseline (dc part) of PPG, and not at all change the pulsatile shape of the PPG signal. Once this aspect is taken care of, the proposed method should not disturb the PPG shape due to the filtering process. In order to show that the proposed method did not change the PPG morphology, the clean PPG signal was processed by AS-LMS, and its merit is shown in Fig. 11. In addition to the visual inspection of Fig. 11, the calculated statistical parameters like root mean square deviation (RMSD) and normalized root mean square error (NRMSE) for the clean section of raw PPG and the AS-LMS-processed clean section, presented in Table IV, establish that fact.

After establishing this, the PPGs corrupted with different MAs were processed. The results of the processing on the PPG data corrupted with typical artifacts are shown in Figs. 12–14. The recovered portions of the MA-reduced PPGs in Figs. 12(e1)–14(e1) clearly indicate the reduction of MA noise components restoring all the required essential morpho-

TABLE IV
COMPUTED RMSD AND NRMSE FOR THE CLEAN SECTION OF PPG

	RMSD	NRMSE (dB)
Cycle 1	0.0744	-8.65
Cycle 2	0.0221	-30.34
Cycle 3	0.3272	-13.13
Cycle 4	0.6890	-10.73
Cycle 5	0.3297	-12.11
Mean ± SD	0.2919 ± 0.267	-15.01 ± 8.73

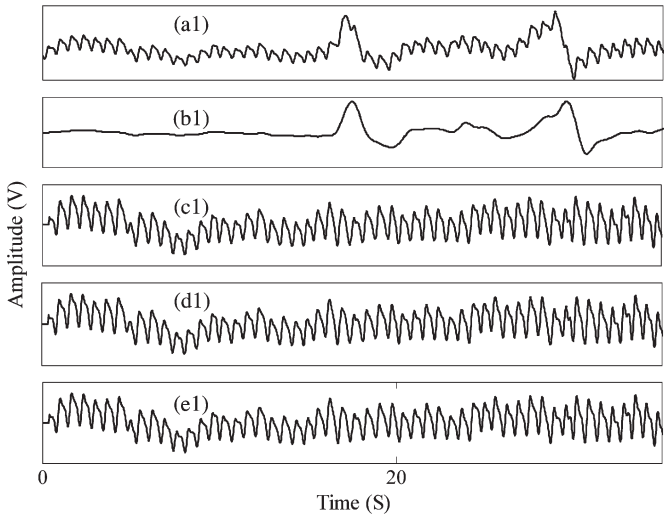

Fig. 12. IR PPG with "vertical motion of finger." (a1) MA-corrupted PPG. (b1) Effective synthetic noise reference signal. (c1) MA-recovered PPG using CS-LMS. (d1) MA-recovered PPG using TVS-LMS. (e1) MA-recovered PPG using AS-LMS.

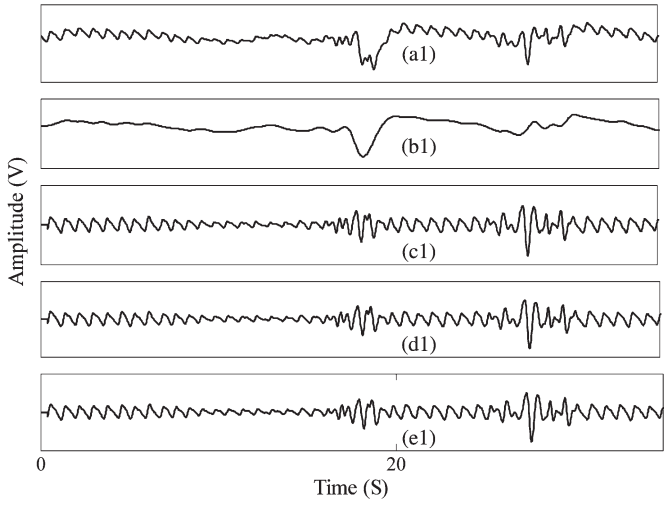

Fig. 13. IR PPG with "bending motion of finger." (a1) MA-corrupted PPG. (b1) Effective synthetic noise reference signal. (c1) MA-recovered PPG using CS-LMS. (d1) MA-recovered PPG using TVS-LMS. (e1) MA-recovered PPG using AS-LMS.

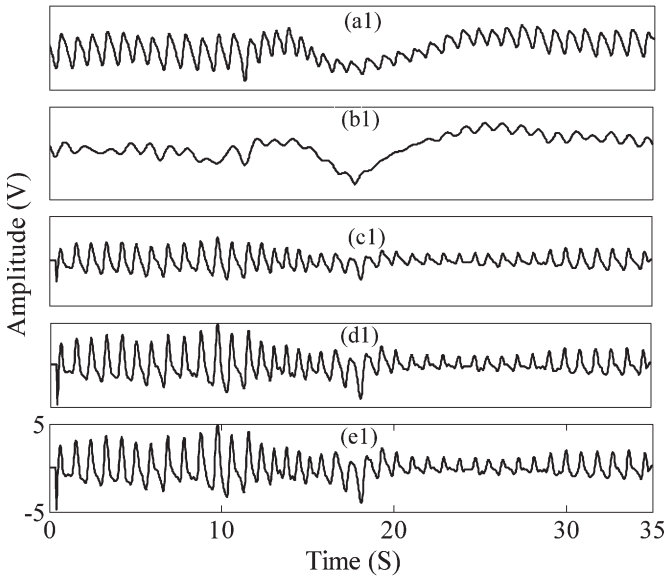

Fig. 14. IR PPG with "horizontal motion of finger." (a1) MA-corrupted PPG. (b1) Effective synthetic noise reference signal. (c1) MA-recovered PPG using CS-LMS. (d1) MA-recovered PPG using TVS-LMS. (e1) MA-recovered PPG using AS-LMS.

logical features of PPG. However, visual inspection of the filtered outputs did not reveal much information about the efficacy of the proposed filtering method. Hence, for performance evaluation of the techniques based on CS-LMS, TVS-LMS, and AS-LMS algorithms, the following statistical analysis was carried out.

1) Peak-to-peak values of the recovered PPG cycles

   The statistical analysis was carried out in terms of mean $\pm$ SD of the peak-to-peak values of every five restored PPG cycles obtained after applying the respective methods on MA-corrupted PPG signals. Results are presented in Table V. The peak-to-peak values of the recovered PPG cycles from the corrupted portions using the AS-LMS algorithm were very close to the clean sections of PPG. For the sake of clarity, whisker plots for the peak-to-peak cycles of MA-corrupted and MA-recovered PPGs are shown in Fig. 15. These efficiently restored peak-to-peak voltage values will be used in the reliable estimation of SpO_2.

2) SNR and NRMSE calculations

   A figure of merit (SNR), defined as the ratio of signal power to the generated noise reference power, was computed for the MA-corrupted and MA-recovered PPG signals. Table VI illustrates the SNR values for the PPGs inflicted with three different kinds of MA. The superiority of AS-LMS is clearly evident in representing high SNR values in all the cases. The deviation of the recovered PPG from the original PPG is quantified by the NRMSE in the reconstructed signal. The NRMSE values of Table VII were calculated using

$$NRMSE = 20\log\left[\sqrt{\sum_{n=0}^{N}\left(S(n)-\hat{S}(n)\right)^2 \Big/ \sum_{n=0}^{N}\left(S(n)\right)^2}\right] \text{ dB} \quad (16)$$

where N represents one period of the recovered PPG cycle. *AS-LMS resulted in good values for NRMSE, indicating that the morphological features of PPG were restored to a large extent compared to other two methods. This may be purely attributed to the ICA method for generating noise reference very close to the actual artifact compared to the FFT and SVD methods, thereby making adaptive filtering very efficient.*

3) Measurement of conventional parameters for digital volume pulse (DVP)

   Once MAs are successfully reduced for restoring the morphological features of PPG, the waveform counteranalysis [31] of PPG was carried out for assessing the arterial stiffness by analyzing the conventional parameters like crest time (CT), stiffness index (SI), reflection index (RI), normalized crest time (NCT), and crest time ratio (CTR). This was performed for different kinds of MAs considered. The evaluated parameters, along with their description, are shown in Fig. 16. and Table VIII.

C. SpO_2 Computation Using TD and FD Analyses

The ultimate goal of the proposed method is to reduce the MAs from PPG for reliable estimation of SpO_2. If MA is detected, most CPOs display previous values of SpO_2 during motion episodes. This issue of displaying previous values is a serious concern for noise-corrupted signals, particularly in the hypoxia status of a patient. Hence, an artifact-free PPG signal that is composed of clearly separable ac and dc parts is highly desired in pulse oximetry. In pulse oximetry, for the measurement of SpO_2, the dc and ac parts of the red and IR PPG signals are to be extracted. If the peak-to-peak values of the pulsatile components of the red and IR PPG signals are AC_{Red} and AC_{IR}, respectively, the "ratio of ratios" R is estimated [4], [27] as

$$\boldsymbol{R} = \frac{(AC_{\mathrm{Red}}/DC_{\mathrm{Red}})}{(AC_{\mathrm{IR}}/DC_{\mathrm{IR}})}. \quad (17)$$

Then, SpO_2 is computed by substituting the R value of (17) in an empirical linear approximate relation given by

$$SpO_2\% = (110 - 25\boldsymbol{R})\%. \quad (18)$$

It has been clearly established in Section IV-B that the AS-LMS adaptive filter efficiently restored the peak-to-peak values of the PPG cycles; SpO_2 is computed using the linear empirical relationship.

In TD analysis, after obtaining the effectively artifact-reduced PPG from the proposed AS-LMS adaptive filter, the normalized R value is calculated from the ac and dc component values of the red and IR PPG signals by measuring the peak-to-peak amplitudes consecutively for every five cycles in the time domain. In addition, spectral analysis was identified as having good potential for improving SpO_2 computation [26]. In FD analysis, the R value is obtained from the spectrum of the recovered PPG signal by tapping the magnitude values at zero frequency (dc) and at cardiac frequency (ac). In FD analysis, nonparametric spectral estimation methods like Periodogram

TABLE V
EFFECTIVENESS OF PROPOSED METHOD IN RESTORING PEAK-TO-PEAK VALUES OF PPG

PPG	Horizontal motion	Vertical motion	Bending motion
Clean Section	0.371± 0.025	0.428± 0.045	0.357± 0.02
Corrupted portion	0.426± 0.087	0.514± 0.107	0.459± 0.067
Recovered portion using CS-LMS	0.388± 0.048	0.443± 0.059	0.364± 0.131
Recovered portion using TVS-LMS	0.379± 0.036	0.435± 0.048	0.359± 0.128
Recovered portion using AS-LMS	0.379± 0.031	0.435± 0.046	0.359± 0.125

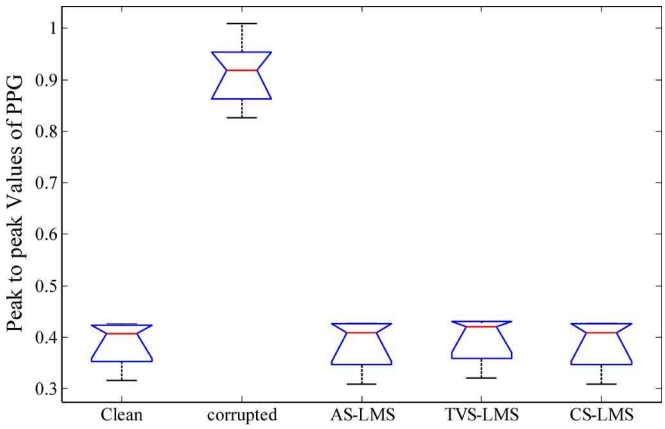

Fig. 15. Whisker plots indicating the restored peak-to-peak values using different LMS algorithms for PPGs corrupted with the vertical motion of the finger. CS-LMS is close to the clean portion.

TABLE VI
COMPUTED VALUES OF SNR FOR MA-CORRUPTED AND MA-RECOVERED PPG SIGNALS FOR DIFFERENT MAS

SNR of PPG	Horizontal motion	Vertical motion	Bending motion
Before Adaptive Filter	1.0745	-5.7089	-5.7414
Using CS-LMS	1.9025	-4.478	-4.2574
Using TVS-LMS	2.3897	-4.1117	-4.0517
Using AS-LMS	2.3890	-4.0012	-4.0494

TABLE VII
COMPUTED VALUES OF NRMSE FOR THE CORRUPTED AND RECOVERED PPGS FOR DIFFERENT MAS

NRMSE of PPG in dB	Horizontal motion	Vertical motion	Bending motion
Using CS-LMS	-1.1280	-0.3408	-0.3734
Using TVS-LMS	-1.1350	-0.3512	-0.3936
Using AS-LMS	-0.8057	-0.3007	-0.3052

method (PM), Bartlett method (BM), Welch method (WM) and Blackman-Tukey method (BTM) are employed for calculating R values by measuring the ac and dc spectral component values

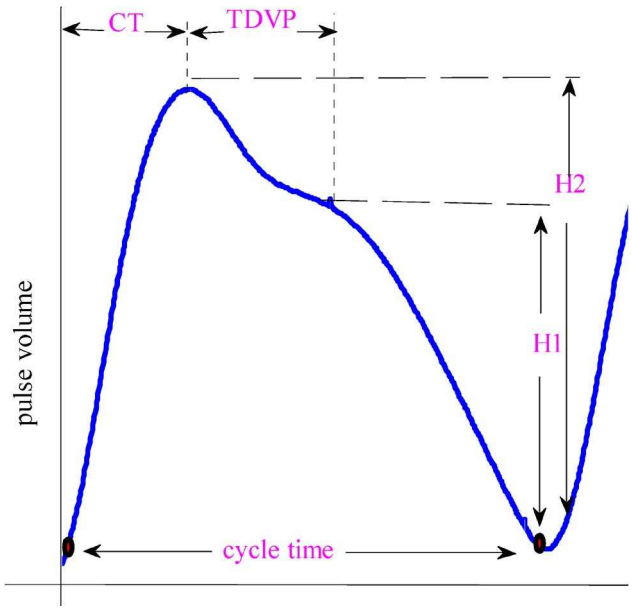

Fig. 16. MA-reduced PPG shown as DVP, indicating conventional parameters for assessing arterial stiffness. Note: *Generally, DVP consists of systolic peak (first peak) and diastolic peak (second peak). The conventional parameters of DVP include: time difference between the first and the second peak (TDVP); stiffness index* (SI) = *bodyheight/TDVP; reflection index* (RI) = *amplitudeof the second peak (H1)/amplitude of the first peak (H2) crest time* (CT) = *the timeinterval from the foot point of wave to the first peak in seconds; normalized crest time* $(NCT) = CT/bodyheight$; *crest time ratio* $(CTR) = CT/cycle\ time$(i.e., *duration from the foot point of one wave to another in seconds).*

from the bar plots shown in Figs. 17 and 18 for both red and IR PPGs only for the case of the vertical motion of the finger.

It was observed that these spectra show considerable difference to various types of MA. The bottom-line advantage of using this method is evident from the results presented in Table IX, wherein the efficacy of the method in restoring the peak-to-peak values of the PPG cycles is demonstrated and which, in turn, results in reliable estimation of SpO_2, as shown in Table X.

Furthermore, the estimated values of SpO_2 before and after processing the PPGs corrupted by the vertical motion of the finger with various test algorithms are shown in Fig. 19. The SpO_2 values using the raw PPGs during the period of MAs fluctuate in a very random manner and are hence unreliable. On

TABLE VIII
CALCULATED CONVENTIONAL PARAMETERS OF MA-REDUCED PPG

PPG conventional parameters assessing arterial stiffness	Vertical motion	Bending motion	Horizontal motion
CT (ms)	190.667	218.33	264.66
TDVP (ms)	180.66	180	175.33
Cycle Time (ms)	662	796.66	924
H1	2.10	2.2	6.27
H2	2.53	2.77	8
SI	11.11	11.11	11.42
RI	0.83	0.794	0.783
NCT	95	109	132
CTR	0.287	0.273	0.285

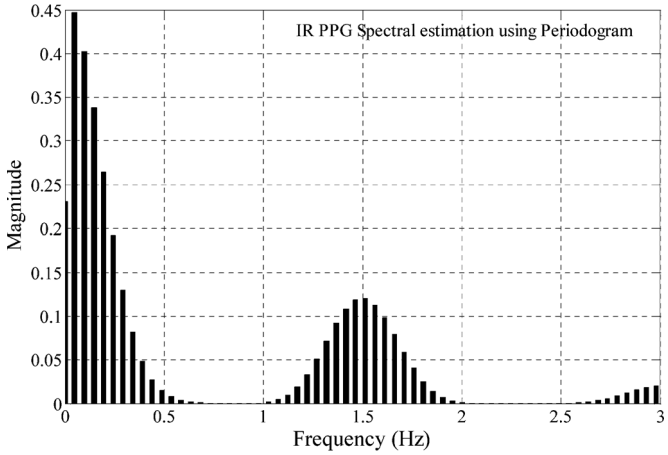

Fig. 17. Estimated spectrum of IR PPG (for vertical motion) using the PM method.

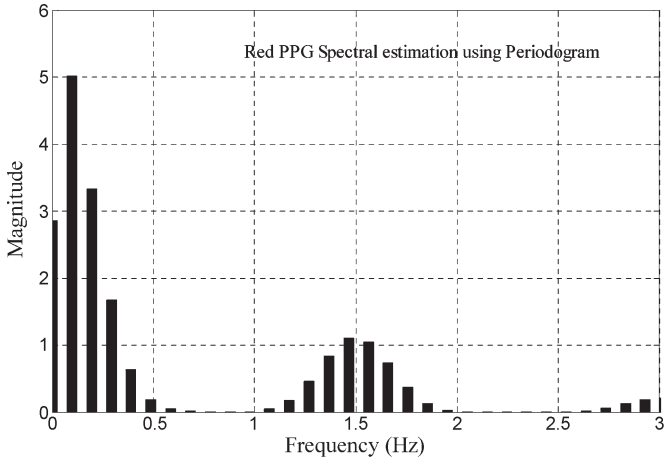

Fig. 18. Estimated spectrum of red PPG (for vertical motion) using the PM method.

the other hand, the SpO_2 values estimated using the PPGs after processing with the presented AS-LMS method deviate very little from the expected values, thus establishing the efficacy of the method in reducing MAs and estimating SpO_2. Hence, the AS-LMS adaptive filter proposed for MA reduction of PPG signals is best suitable for the present-day PPG sensor head of CPO.

TABLE IX
COMPUTED **R** VALUES IN BOTH TIME AND FREQUENCY DOMAINS

PPG	Computed *R* value in TD	Computed *R* value in FD			
		PM	BM	WM	BTM
Clean section	0.48±0.02	0.56±0.04	0.56±0.06	0.54±0.05	0.48±0.04
Bending motion	0.56±0.15	0.64±0.52	0.64±0.58	0.60±0.21	0.56±0.26
Vertical motion	0.48±0.06	0.60±0.009	0.56±0.06	0.48±0.05	0.48±0.04
Horizontal motion	0.60±0.14	0.64±0.47	0.68±0.24	0.64±0.27	0.60±0.18

TABLE X
ESTIMATED SpO_2 FROM MA-RECOVERED PPG

PPG	SpO_2 from TD Analysis	SpO_2 from FD Analysis			
		PM	BM	WM	BTM
Clean section	98%	96%	96%	97%	98%
Bending motion	96%	94%	94%	95%	96%
Vertical motion	98%	95%	96%	98%	98%
Horizontal motion	95%	94%	93%	94%	95%

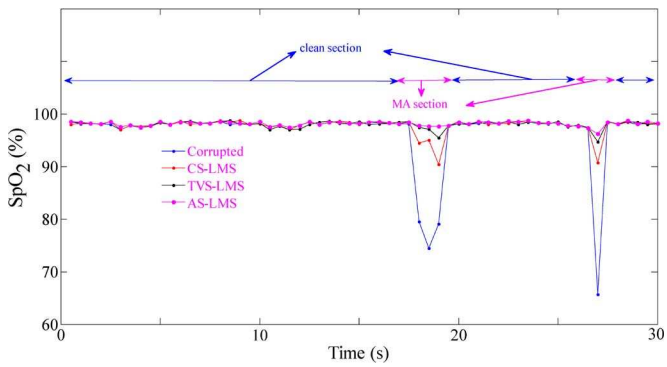

Fig. 19. Estimated SpO_2 for raw PPGs corrupted with the vertical motion of the finger and processed PPGs using CS-LMS, TVS-LMS, and AS-LMS.

V. CONCLUSION

In this paper, we have presented a simple yet efficient filtering method based on an AS-LMS adaptive filter for MA reduction in corrupted PPG signals. In general, the MA reduction methods developed using adaptive filters invariably depend on additional hardware for acquiring noise reference signal. The novelty of the method lies in the fact that a synthetic noise reference signal, representing MA, is generated from the corrupted PPG itself, for use in adaptive filtering, without using any additional hardware. For validation of the generated noise reference signal before applying to the adaptive filter, three different methods, namely, FFT, ICA, and SVD, are utilized individually for generation of noise reference signal, and their correlation with the MA noise component is tested. Although the criterion used for the selection of the best synthetic noise reference signal generated (by using FFT, SVD, and ICA methods) was the method which yielded the noise reference signal with the highest values for both skew and kurtosis, a high value of kurtosis alone would serve as a reliable measure for

the selection of synthetic noise reference signal. Fast convergence of AS-LMS compared to both TVS-LMS and CS-LMS techniques, in addition to restoring the peak-to-peak values of the PPG cycles by it, resulted in efficient reduction of MAs from the PPG signals. The test results on the recorded PPG signals with frequently encountered motions proved the efficacy of the presented filtering method for reliable and accurate estimation of SpO_2 values, thus making the method best suitable for present-day CPOs utilizing the existing two-wavelength sensor probe without any additional hardware. In addition to SpO_2 estimation, the waveform contour analysis was done on artifact-reduced PPG, and the conventional parameters were evaluated for assessing the arterial stiffness.

ACKNOWLEDGMENT

The authors would like to thank the reviewers of this paper and of the IEEE International Instrumentation and Measurement Technology Conference (I^2MTC) paper [25], whose critical reviews and suggestions enabled them to improve the contents of this paper. The authors would also like to thank Prof. V. Jagadeesh Kumar, Department of Electrical Engineering, IIT Madras, India, for the valuable suggestions and encouragement.

REFERENCES

[1] E. N. Bruce, *Biomedical Signal Processing and Signal Modeling*. New York: Wiley, 2001.

[2] J. G. Webster, *Design of Pulse Oximeters*. New York: Taylor & Francis, 1997.

[3] Y. Mendelson and B. Ochs, "Noninvasive pulse oximetry utilizing skin reflectance photoplethysmography," *IEEE Trans. Biomed. Eng.*, vol. 35, no. 10, pp. 798–805, Oct. 1988.

[4] K. A. Reddy, "Novel methods for performance enhancement of pulse oximeters," Ph.D. dissertation, Dept. Elect. Eng., IIT Madras, Chennai, India, 2008.

[5] T. L. Rusch, R. Sankar, and J. E. Scharf, "Signal processing methods for pulse oximetry," *Comput. Biol. Med.*, vol. 26, no. 2, pp. 143–159, Mar. 1996.

[6] A. B. Barreto, L. M. Vicente, and I. K. Persad, "Adaptive cancellation of motion artifact in photoplethysmographic blood volume pulse measurements for exercise evaluation," in *Proc. IEEE-EMBC/CMBEC*, Sep. 20–23, 1995, vol. 2, pp. 983–984.

[7] A. R. Relente and L. G. Sison, "Characterization and adaptive filtering of motion artifacts in pulse oximetry using accelerometers," in *Proc. Conf. EMBS/BMES*, Houston, USA, Oct. 23–26, 2002, pp. 1769–1770.

[8] K. W. Chan and Y. T. Zhang, "Adaptive reduction of motion artifact from photoplethysmographic recordings using a variable step-size LMS filter," in *Proc. IEEE Sens.*, 2002, vol. 2, pp. 1343–1346.

[9] F. M. Coetzee and Z. Elghazzawi, "Noise-resistant pulse oximetry using a synthetic reference signal," *IEEE Trans. Biomed. Eng.*, vol. 47, no. 8, pp. 1018–1026, Aug. 2000.

[10] J. M. Goldman, M. T. Petterson, R. J. Kopotic, and S. J. Barker, "Masimo signal extraction pulse oximetry," *J. Clin. Monit. Comput.*, vol. 16, no. 7, pp. 475–483, Sep. 2000.

[11] J. Lee, W. Jung, I. Kang, Y. Kim, and G. Lee, "Design of filter to reject motion artifact of pulse oximetry," *Comput. Stand. Interfaces*, vol. 26, no. 3, pp. 241–249, May 2004.

[12] C. M. Lee and Y. T. Zhang, "Reduction of motion artifacts from photoplethysmographic recordings using a wavelet denoising approach," in *Proc. IEEE EMBS Asian-Pacific Conf. Biomed. Eng.*, 2003, pp. 194–195.

[13] Y. S. Yan, C. C. Poon, and Y. T. Zhang (2005, Mar.). Reduction of motion artifact in pulse oximetry by smoothed pseudo Wigner–Ville distribution. *J. Neuro. Eng. Rehabil.* [Online]. *(1)*, p. 3. Available: http://www.jneuroengrehab.com/content/2/1/3

[14] M. J. Hayes and P. R. Smith, "Artifact reduction in photoplethysmography," *Appl. Opt.*, vol. 37, no. 31, pp. 7437–7446, Nov. 1998.

[15] M. J. Hayes and P. R. Smith, "A new method for pulse oximetry possessing inherent insensitivity to artifact," *IEEE Trans. Biomed. Eng.*, vol. 48, no. 4, pp. 452–461, Apr. 2001.

[16] P. F. Stetson, "Independent component analysis of pulse oximetry signals," in *Proc. 26th Annu. Int. Conf. IEEE Eng. Med. Biol. Soc.*, San Francisco, CA, Sep. 1–5, 2004, pp. 231–234.

[17] B. S. Kim and S. K. Yoo, "Motion artifact reduction in photoplethysmography using independent component analysis," *IEEE Trans. Biomed. Eng.*, vol. 53, no. 3, pp. 566–568, Mar. 2006.

[18] J. Yao and S. Warren, "A short study to assess the potential of independent component analysis for motion artifact separation in wearable pulse oximeter signals," in *Proc. 27th Annu. Conf. IEEE Eng. Med. Biol.*, Shanghai, China, Sep. 1–4, 2005, pp. 3585–3588.

[19] J. Y. A. Foo, "Comparison of wavelet transformation and adaptive filtering in restoring artifact-induced time-related measurement," *Biomed. Signal Process. Control*, vol. 1, no. 1, pp. 93–98, Jan. 2006.

[20] K. A. Reddy and V. J. Kumar, "Motion artifact reduction in photoplethysmographic signals using singular value decomposition," in *Proc. 24th IMTC*, Warsaw, Poland, May 1–3, 2007, pp. 1–4.

[21] K. A. Reddy, B. George, and V. J. Kumar, "Use of Fourier series analysis for motion artifact reduction and data compression of photoplethysmographic signals," *IEEE Trans. Instrum. Meas.*, vol. 58, no. 5, pp. 1706–1711, May 2009.

[22] R. Krishnan, B. Natarajan, and S. Warren, "Two-stage approach for detection and reduction of motion artifacts in photoplethysmographic data," *IEEE Trans. Biomed. Eng.*, vol. 57, no. 8, pp. 1867–1876, Aug. 2010.

[23] M. R. Ram, K. V. Madhav, E. H. Krishna, K. N. Reddy, and K. A. Reddy, "Adaptive reduction of motion artifacts from PPG signals using a synthetic noise reference signal," in *Proc. IEEE EMBS Conf. Biomed. Eng. Sci.*, Nov./Dec. 2010, pp. 315–319.

[24] M. R. Ram, K. V. Madhav, E. H. Krishna, K. N. Reddy, and K. A. Reddy, "On the performance of time varying step-size least mean squares (TVS-LMS) adaptive filter for MA reduction from PPG signals," in *Proc. IEEE Int. Conf. Commun. Signal Process.*, Feb. 2011, pp. 431–435.

[25] M. R. Ram, K. V. Madhav, E. H. Krishna, K. N. Reddy, and K. A. Reddy, "On the performance of AS-LMS based adaptive filter for reduction of motion artifacts from PPG signals," in *Proc. 28th I2MTC*, Hangzhou, China, May 10–12, 2011, pp. 1536–1539.

[26] V. K. Madisetti and D. V. Williams, *Digital Signal Processing Hand Book*. Boca Raton, FL: CRC Press, 1999.

[27] K. A. Reddy, B. George, N. M. Mohan, and V. J. Kumar, "A novel calibration-free method for measurement of oxygen saturation in arterial blood," *IEEE Trans. Instrum. Meas.*, vol. 58, no. 5, pp. 1699–1705, May 2009.

[28] S. Rhee, B. H. Yang, and H. H. Asada, "Artifact-resistant power-efficient design of finger-ring plethysmographic sensors," *IEEE Trans. Biomed. Eng.*, vol. 48, no. 7, pp. 795–805, Jul. 2001.

[29] H. H. Asada, H. H. Jiang, and P. Gibbs, "Active noise cancellation using MEMS accelerometers for motion-tolerant wearable bio-sensors," in *Proc. 26th Annu. Int. Conf. IEEE EMBS*, San Francisco, CA, Sep. 1–5, 2004, pp. 2157–2160.

[30] P. Gibbs and H. H. Asada, "Reducing motion artifact in wearable bio-sensors using MEMS accelerometers for active noise cancellation," in *Proc. Amer. Control Conf.*, Portland, OR, USA, Jun. 8–10, 2005, pp. 1581–1586.

[31] H. T. Wu, C. C. Liu, P. H. Lin, H. M. Chung, M. C. Liu, H. K. Yip, A. B. Liu, and C. K. Sun, "Novel application of parameters in waveform contour analysis for assessing arterial stiffness in aged and atherosclerotic subjects," *J. Atherosclerosis*, vol. 213, no. 1, pp. 173–177, Nov. 2010.

M. Raghu Ram (M'11) was born in Khammam, India, in 1977. He received the B.E. degree from Osmania University, Hyderabad, India, in 1999 and the M.Tech. degree from Jawaharlal Nehru Technological University (JNTU), Kakinada, India, in 2008.

He is a Research Scholar at JNTU, Hyderabad, and is currently an Associate Professor with the Department of Electronics and Instrumentation Engineering, Kakatiya Institute of Technology and Science, Warangal, India. His research interests include biomedical instrumentation, digital signal processing, and instrumentation.

K. Venu Madhav (M'10) was born in Nizamabad, India, in 1975. He received the B.E. degree of Dr. Babasaheb Ambedkar Marathwada University, Aurangabad, India, in 1997 and the M.Tech. degree from Jawaharlal Nehru Technological University (JNTU), Kakinada, India, in 2008.

He is a Research Scholar at JNTU, Hyderabad, and is currently an Associate Professor with the Department of Electronics and Instrumentation Engineering, Kakatiya Institute of Technology and Science, Warangal, India. His research interests include instrumentation, biomedical instrumentation, digital signal processing.

E. Hari Krishna (M'11) was born in Warangal, India, in 1983. He received the B.Tech. degree from Jawaharlal Nehru Technological University (JNTU), Hyderabad, India, in 2004 and the M.Tech. degree from Kakatiya University (KU), Warangal, in 2009.

He is a Research Scholar at JNTU, Hyderabad, and is currently an Assistant Professor with the Department of Electronics and Communication Engineering, KU College of Engineering and Technology, KU. His research interests include biomedical instrumentation, digital signal processing, and signal processing for communication.

Nagarjuna Reddy Komalla was born in Warangal, India, in 1968. He received the Bachelor degree in medicine from the NTR University of Health Sciences (NTRUHS), Vijayawada, India, in 1993 and the M.D. degree in anaesthesiology from Osmania Medical College, NTRUHS, in 1999.

He is currently an Assistant Professor with the Department of Anaesthesiology, Govt. MGM Hospitals, Warangal. His clinical interests include critical care and pain management, and his research interest includes painless labor.

K. Ashoka Reddy (M'12) was born in Warangal, India, in 1970. He received the B.Tech. degree from Kakatiya University, Warangal, in 1992, the M.Tech. degree from Jawaharlal Nehru Technological University, Kakinada, India, in 1994, and the Ph.D. degree in electrical engineering from the Indian Institute of Technology Madras, Chennai, India, in 2008.

He is currently a Professor with the Department of Electronics and Instrumentation Engineering, Kakatiya Institute of Technology and Science, Warangal. His research interests include instrumentation, biomedical signal processing, and signal processing for communication.